Journal of Physics: Conference Series **514** (2014) 012024 doi:10.1088/1742-6596/514/1/012024

Noble metallic nanostructures: preparation, properties, applications

P A Atanasov[1,5], N N Nedyalkov[1], A Og Dikovska[1], Ru Nikov[1], S Amoruso[2,3], X Wang[3], R Bruzzese[2,3], K Hirano[4], H Shimizu[4], M Terakawa[4] and M Obara[4]

[1]Institute of Electronics, Bulgarian Academy of Sciences, 72 TsarigradskoChaussee, 1784 Sofia, Bulgaria
[2]Dipartimento di Scienze Fisiche, Università degli Studi di Napoli Federico II, Complesso Universitario di Monte S. Angelo, Via Cintia, I-80126 Napoli, Italy
[3]CNR-SPIN, Complesso Universitario di Monte S. Angelo, Via Cintia, I-80126, Napoli, Italy
[4]School of Integrated Design Engineering, Keio University, 3-14-1, Hiyoshi, Kohoku-ku, Yokohama-shi, 223-8522, Japan

E-mail: paatanas@ie.bas.bg

Abstract. The process of formation and the characteristics are studied of noble metal nanostructures created by pulsed laser ablation in vacuum. Femtosecond (fs) and nanosecond (ns) laser systems lasing at different wavelengths are used. Several different modifications of the pulsed lased deposition (PLD) technique, as off-axis deposition and glancing angle deposition configurations are used to create nanostructures. Laser annealing of single or bimetal thin films is used to fabricate alloyed nanostructures. The possibility is demonstrated of tuning the optical properties of gold nanostructures on flexible substrates. Different experimental techniques, as fast photography, optical emission spectroscopy, FE-SEM, AFM, TEM, and Raman spectroscopy are applied to characterize the noble metallic nanostructures produced. The optical spectra of the Au and Ag nanostructures are also studied experimentally and theoretically. The theoretical simulation methods used are: molecular dynamic (MD), finite difference time domain (FDTD) and a method based on the generalized multi-particle Mie (GMM) theory. Applications of noble metal nanostructures to surface enhanced Raman spectroscopy (SERS) and biophotonics are briefly considered.

1. Introduction

The properties of the noble metal nanostructures have been the object of considerable fundamental and technological interest. The excitation spectrum of noble metallic sub-wavelength structures is determined by its surface plasmon resonances. The energies of plasmon resonances depend strongly on the shape and composition of the nanostructure. The tunability of the plasmon resonances of noble metallic nanoparticles can be exploited to position the optical resonances at specific wavelength regions of interest and has led to a wide range of applications. The strong local electro-magnetic field enhancement accompanied by the surface plasmon resonances has also been used to manipulate light-

[5] To whom any correspondence should be addressed.

matter interactions; noble metallic sub-wavelength structures have been widely applied to surface enhanced Raman spectroscopy (SERS). In addition to their fundamental importance, plasmonic nanostructures have received a great deal of attention for their potential applications in areas such as sub-wavelength waveguides, optical nanoantennas, photovoltaic technology for efficient light coupling into solar cells, metamaterials, chemical and biological sensing, and in biomedical applications.

The interaction of intense nanosecond (ns) or femtosecond (fs) laser pulses with solid targets has generated a lot of interest in recent years due to the variety of possibilities offered both to basic science and technology. The use of fs laser pulses opens up the possibility to decouple the initial photo-excitation of the target from the subsequent dynamics of the removed material, in contrast with the case of longer pulses (ns). In the former case, the pulse width is less than the typical electron-lattice thermalization time, which is ~ few ps. And finally, the irradiated material is driven into an extremely excited state followed by a rapid quenching, which results in a material blow-off composed of fast ions and atoms as well as clusters and nano-aggregates of the target material, depending on the processing parameters. Fs-laser ablation of metals and semiconductors in a vacuum environment has been investigated extensively. Recent research has in particular been focused on the formation mechanism of nanoparticles (NPs) created by the irradiation of a solid target by intense fs laser pulses of different duration in vacuum [1–4].

As a result of the progress in nanotechnologies during the last two decades, nanosystems find nowadays application in many areas, such as chemistry, optics, biology, medicine, microelectronics, etc. This multilateral usage of the NPs in their quality of fundamental structures in nanotechnology, is based on their unique properties, differing considerably from those of bulk materials. The appearance of characteristic bands in the absorption spectra of metallic NPs is related to the electron gas excited by light oscillations. For noble metals (Ag, Au), these bands are in the visible and near UV region. The collective oscillations of electrons are sensitive to the NPs size, shape and surrounding medium. Both Ag and Au NPs have attracted intensive interest because of peculiarities in their absorptrion spectra in the region of the surface plasmon resonance and the specific and very important applications in nanobiotechnology.

The purpose of this paper is to describe the development of several methods for generating noble metal nanostructures. Ns and fs laser ablation of solid metal targets or thin films in vacuum is studied and used, respectively, to manipulate the production of nanostructures. Moreover, results on laser annealing of single or bimetal thin films for fabrication of alloyed nanostructures are also presented. Tuning of the optical properties of gold nanostructures fabricated on flexible substrates is also demonstrated. The properties of the structures produced are experimentally characterized by a variety of methods, as fast photography, optical emission spectroscopy, FE SEM, AFM, TEM, Raman spectroscopy. Moreover, molecular dynamic (MD) simulation, finite difference time domain (FDTD) and a method based on the generalized multiparticle Mie theory (GMMT) are applied and the results are compared with the experimental ones. Three possible applications of the Au NPs are briefly described, namely, SERS, photothermal cancer cell therapy and plasmonic nanometric optical tweezers.

2. Experimental

Two laser systems are used in the experiments. The fs laser system consists of a Nd: Glass laser lasing at λ = 1055 nm ($\tau_p \approx$ 0.9 ps and rep rate 33 Hz), SHG - λ = 527 nm ($\tau_p \approx$ 300 fs) and FHG - λ = 263nm ($\tau_p \approx$ 300 fs), respectively. The second experimental set up used is based on a ns Nd:YAG laser working at λ = 1064, 532, 355 or 266 nm (τ_p = 15 ns and rep rate 10 Hz).

The experimental study of the plume and its evolution in time in vacuum are described in detail in [3, 5-7]. Briefly, the optical emission from the ablation plume is collected along an axis perpendicular to the target surface normal and imaged onto the entrance slit of a spectrograph coupled to an intensified charge-coupled device camera. The evolution of the emitting species inside the expanding plume is followed by measuring their emission spectra at different time delays with respect to the arrival time of the laser pulse on the target, and at different distances from the target surface. Fast

photography is applied to follow the vacuum expansion dynamics of the ablated species. The morphology of the deposited NPs is analyzed by AFM or SEM and the shape of the NPs is viewed by TEM. XRD and EDS analyses are performed to check the elemental properties of the NPs.

3. Theoretical

The numerical model is based on the classical MD simulation technique together with two-temperature (2T) modeling. Details are given elsewhere [3, 5-8]. A Morse potential is used to describe the interaction between the particles, and its specific parameters are taken from Ref. [9]. In order to simulate an infinite material in lateral directions, periodic boundary conditions are imposed in the *x–y* directions. Specific boundary conditions are applied to the bottom of the computational cell in order to prevent the reflection of shock waves [10]. The laser energy absorption and the heat redistribution into the metal is governed initially by the free electrons. Since the electrons are not included explicitly in the MD model, their role, and the heating of the material, is taken into account by using the one dimensional 2T diffusion model. The temperature into the material predicted by the two temperature model is implemented in the MD by way of scaling the atoms' velocities.

The interaction of light with the metal nanoobjects can be simulated by the FDTD approach [11,12]. It has recently become a state-of-the-art method for solving Maxwell's equations in complex geometries, variety of materials and environments. Being a direct time and space solution, it offers the user a unique insight into all types of problems in electromagnetism and photonics. Using the FDTD algorithm is necessary when the characteristic sizes are in the order of the wavelength.

The near-field properties around a metallic particle can be described by the Mie scattering theory [13]. Mie theory, also called Lorenz-Mie theory or Lorenz-Mie-Debye theory, is an analytic solution of Maxwell's equations for the scattering of electromagnetic radiation by spherical particles (also called Mie scattering). Mie theory provides rigorous analytic solutions for light scattered by an isotropic sphere embedded in a homogeneous medium.

4. Control of the nanostructure's properties

We have developed several methods for producing noble metal nanostructures and manipulating their properties – size distribution, shape and composition. One of the important parameters for controlling the size or size distribution of the NPs produced in vacuum is the photon energy (laser wavelength) of the laser radiation used for ablation. This was proven in the case of laser ablation of a solid target by fs pulses [6]. In particular, the size distribution of the NPs is quite broad in the case of visible light (527 nm), and becomes significantly narrower and slightly shifted towards smaller sizes for ultraviolet light (263 nm). This concept being only verified theoretically and experimentally in the case of Ni notwithstanding, we assumed that the laser wavelength is an effective parameter in controlling the NPs size distribution in fs laser ablation of other metals.

4.1. Ultrafast-laser ablation of thin gold film targets

A way to control the size of the nanoparticles is proposed in [14]. Fs-laser ablation of a Au thin film is studied in order to create NPs and compared with that of the bulk target. The experimental results are confirmed by MD simulation of the process and by optical spectroscopy of the plumes. A reduction of the NPs size and a narrowing by a factor two of their size distribution in the case of ablation of a thin film target is observed – figure 1. This fact is attributed to the more uniform heating of the target material – thin film compared to the bulk material – figure 2. In addition, a significant difference is observed between the two cases in terms of the plume's expansion dynamics. Thus, ultrashort-laser ablation of thin films provides a promising way of controlling the plume's characteristics and the NPs size.

4.2. Nanosecond pulsed laser deposition of thin films and laser heating

A method is developed for production of Au and Ag nanostructures which consists of two steps: 1st one – PLD of a thin (50÷100 nm) metal film and 2nd – laser annealing with ns pulses [15]. At certain conditions, the annealing leads to a homogeneous decomposition of the film into NPs with diameters

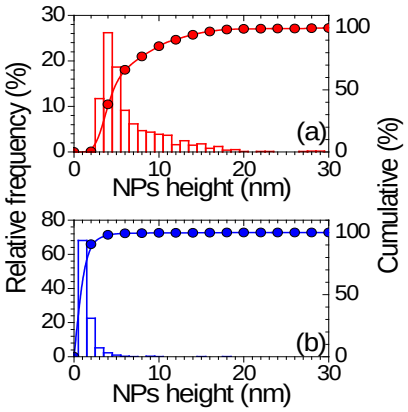

Figure 1. Size histogram and cumulative distribution of the NPs height produced by ultrashort laser ablations of (a) a Au bulk target, and (b) a Au thin film. The thickness of the thin film is 100 nm.

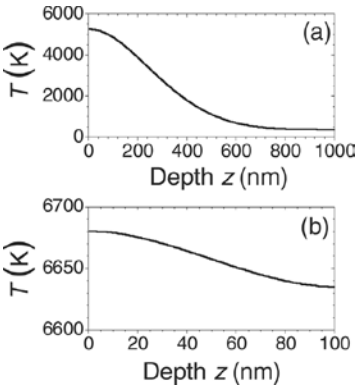

Figure 2. Temperature profiles for a Au target obtained by one-dimensional 2T diffusion model calculated at 40 ps after the laser pulse: (a) bulk material; (b) 100 nm thick film. The scales of z are different in plots (a) and (b).

in the range of few tens of nanometers – figure 3. The fragmentation into droplets occurs if the liquid phase wets poorly the substrate. This is a relatively simple way to produce metal NPs on different substrates. The nanostructured surfaces fabricated can be used successfully as substrates for SERS analyses.

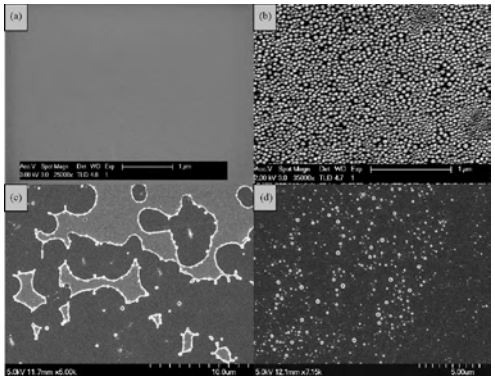

Figure 3. SEM images of a Au thin film with a thickness of d ~ 60nm annealed at a fixed number of pulses (10): (a) - as deposited film; (b) - annealed at F = 130 mJ/cm^2, (c) – F = 200 mJ/cm^2; and (d) - F = 300 mJ/cm^2.

4.2.1. Different modifications of ns-pulsed laser deposition of nanostructures. Two different experimental modifications of ns-pulsed laser deposition are applied in order to create Au, Ag or ZnO nanorods – off-axis PLD and deposition at glancing angle of the plume with respect to the substrate (GLAD) configurations.

Using off-axis PLD, where the target center is at a distance of 1÷2 cm from the plume's axis, ZnO nanorods grow when Au NPs are initially deposited on the substrate [16]. The experimental conditions are: HG or FHG Nd:YAG laser with energy density of ~3.5 J/cm^2, substrate temperature T_s = 0°C or 150°C and oxygen pressure in the chamber P_{O2} = 5 Pa. These Au NPs act as growth nuclei – figure 4.

Figure 5 depicts Au nanocolumns grown in a GLAD configuration. The glancing angle between the substrate surface and the plume axis is $\alpha \sim 5^o$. As is seen, the nanocolumns are parallel are inclined at a small angle with respect to the substrate's surface normal. Some of these structures are successfully used in the SERS experiments after covering with a thin Au film (~ 5 nm).

4.2.2. Fabrication of alloyed nanostructures. A technique is developed for fabricating alloyed nanostructures [17] allowing one to control and manipulate the optical properties of the nanostructures produced. The films are deposited by the classical on-axis PLD technology using targets consisting of

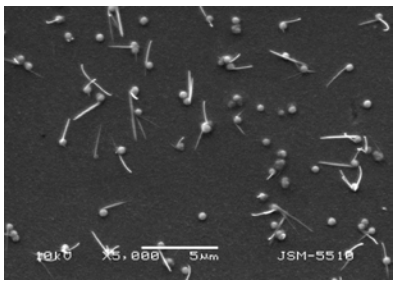

Figure 4. SEM image of ZnO nanorods grown using 200 nm Au NPs (as growth nuclei) at 150 C substrate temperature during deposition.

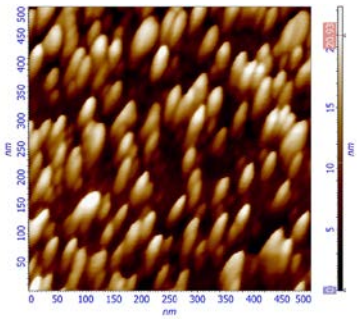

Figure 5. AFM images of Au nanocolumns grown at a GLAD configuretion and Nd: YAG laser THG at 1 J/cm^2 and room temperature.

two sections composed by different metals. Au/Ni or Au/Ag thin films are thus deposited on quartz substrates. By changing the area of the different sections of the target, thin alloyed films with different concentrations of the two metals are obtained. The concentration in the films affects the optical behavior of the films (experimentally obtained extinction spectra) – figure 6. As it is seen, the optical spectra (extinction) depend strongly on the ratio of the elements' concentration.

The average particle diameter in all samples (film thickness of ~80 nm) is in the range between 50 and 30 nm; the size decreases with the increase of the laser fluence. The structures fabricated exhibit a pronounced plasmon resonance behavior in the optical spectra. In combination with a magnetic material, as in the case of Au/Ni structures, a possibility will be open for the development of new technologies in the magneto-optics and spintronics.

4.2.3. Ns-pulsed laser deposition and Ns-annealing of noble metal nanostructures on polymers. An interesting approach is to deposit noble-metal thin films on polymers, then anneal them thus creating 2D or 3D nanostructures [18]. The problem encountered here is the low melting or burning points of the polymers. Bending the flexible substrate will change the distance between the NPs and, thus, tune the optical properties of the structure. Figure 7 presents SEM images of gold nanostructures produced on PMMA and PVC substrates.

Bending the substrate in the range 0÷1,5 mm results in a continuous change of the position of the transmission minimum by ~ 30 nm. The influence of the structure's geometry change on its optical spectra has to do with the change of the inter-grain distance, which affects significantly the optical properties of system via plasmon coupling and multimode plasmon excitation – figure 8.

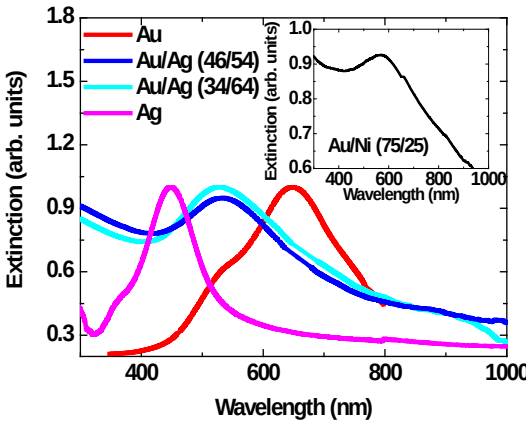

Figure 6. Extinction spectra of Au, Ag and Au/Ag alloy structures. The inset depicts the extinction spectra of a Au/Ni structure. The films deposited are annealed by 5 ns pulses at a fluence of 470 mJ/cm^2. The numbers in brackets indicate the composition in atomic percents.

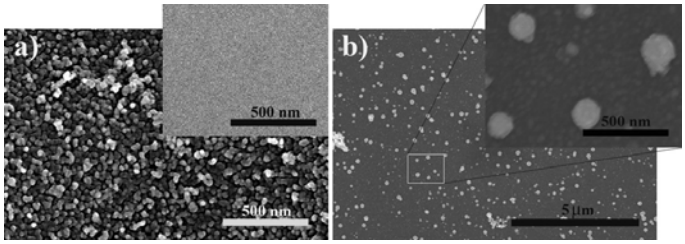

Figure 7. SEM images of Au nanostructures on: a) PMMA and b) PVC substrates. Annealing by a single pulse at F = 90 mJ/cm^2 is used. Insets a) as-deposited Au film on PMMA; b) a detailed view of the structure.

5. Application of gold nanostructures

We present three possible advanced applications of Au nanostructures in SERS spectroscopy, photothermal HeLa cancer cell therapy and development of plasmonic nanometric optical tweezers in an asymmetric gap on Au nanostructured substrates.

5.1. Application of gold nanostructures to SERS spectroscopy

Gold nanostructures produced by the different modification methods described above are successfully applied to SERS spectroscopy. As an example, the Raman spectrum of Rhodamine 6G (R6G) on Au nanocolumns produced by a modified GLAD PLD technology (figure 5) is presented in figure 9 a). Figure 9 b) shows Raman spectra of R6G-covered gold nanostructures and a Au thin film produced on PVC. Obviously, no enhancement is present in the case of the gold film (blue line in figure 9 b). Generally, the Raman spectrum of R6G at a concentration as low as 1 nM is measured [19]. The maximal field-enhancement effect induced by surface plasmon polaritons of Au-nanostructured surfaces exceeds 10^5.

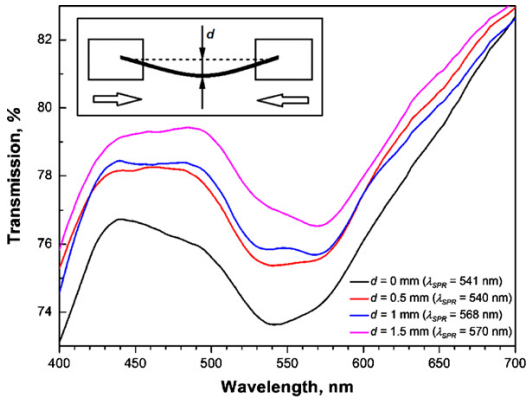

Figure 8. Dependence of the optical transmission spectra of a Au nanostructure on a PMMA substrate on the degree of bending. The as-deposited Au film is annealed by 5 pulses at F = 90 mJ/cm^2. The inset shows the experimental setup for the bending experiments. λ_{SPR} is the wavelength of the transmission minimum.

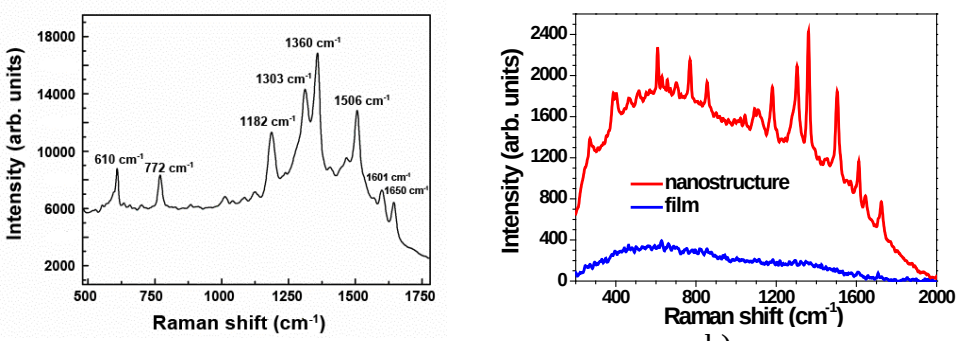

a) b)

Figure 9. Enhanced Raman spectra of R6G covering: a) nanocolumns produced by a modified GLAD PLD technology; b) red line – spectrum of Au NPs produced by PLD on a polymer and subsequently annealed (the structure is the same as in figure 7 b); blue line – spectrum of an as-deposited Au thin film. The R6G concentrations are equal.

5.2. Nanosecond laser heating of Au nanoparticles: application in photothermal cancer cell therapy

The effect is studied of gold nanoparticles with diameters between 40 and 200 nm on several types of cancer cells [20]. Based on the Mie scattering theory, the optimal conditions of particle absorption at different wavelengths in the visible spectrum are estimated. The absorption cross-sections calculated are used in th 2D heat-diffusion equation to describe the heating process of the particle and the surrounding medium. Using this model, the dependence is obtained of the maximal particles' temperature reached on the laser fluence applied. Figure 10 shows a TEM image of a HeLa tumor cell with Au NPs and optical spectra of this NPs configuration.

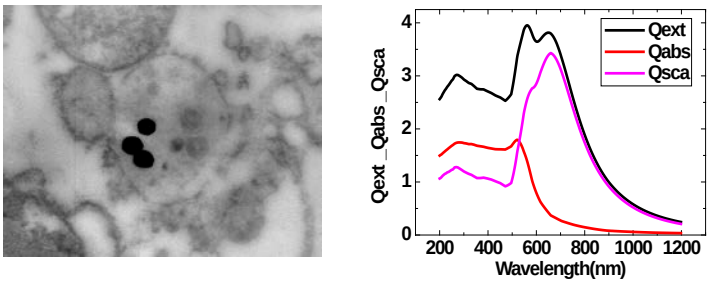

Figure 10. TEM image of a slice of a HeLa tumor cell with deposited gold NPs with diameter of 100 nm and the calculated optical spectra of the system.

Figure 11 a) and b) present the HeLa cell viability after nanoparticle-assisted photothermal treatment. The influence is seen of the Au NPs diameter on the cytotoxic effect – the maximum effect is achieved for 100 nm (fgure 10). Moreover, HeLa cell viability decreases with the increase of the laser fluence – figure 11 b). Further experiments are needed to clarify these effects.

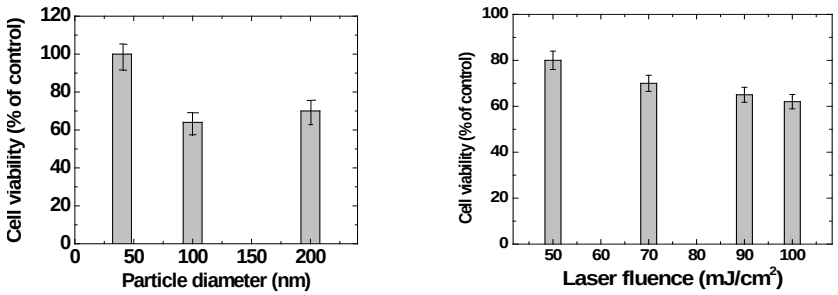

a) b)

Figure 11. a) HeLa cell viability after NP-assisted photothermal treatment at a laser fluence of 90 mJ/cm^2 and irradiation time of 5 s. b) HeLa cell viability as a function of laser fluence at irradiation time of 5 s. The nanoparticles' diameters are 100 nm. The viability is estimated 6 hours after the laser treatment.

5.3. Plasmonic nanometric optical tweezers in an asymmetric space of Au nanostructured substrates
A possible application of Au nanoparticles is proposed [21], namely, plasmonic near-field tweezers in water with gold nanosphere pairs on various substrates. The enhanced near field (figure 12) localized in the nanometric gap pumped by fs laser light (800 nm) linearly-polarized along the axis between thee nanosphere pair can trap and kill small viruses.

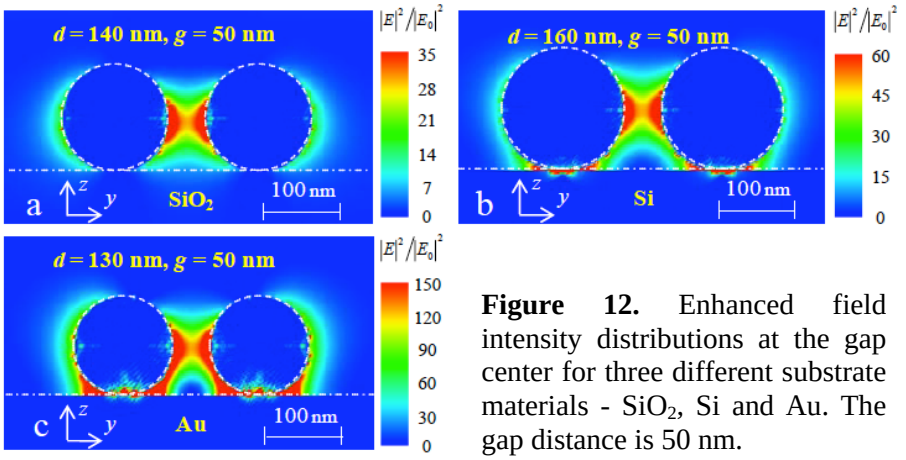

Figure 12. Enhanced field intensity distributions at the gap center for three different substrate materials - SiO_2, Si and Au. The gap distance is 50 nm.

The maximal optical trapping force obtained is larger than 20 pN at an incident optical peak intensity of 1 mW/μm^2. In the system, the enhanced near field stems mainly from the image charge effect, exhibiting an optical trapping in an asymmetric space. The trapped viruses may easily be inactivated using an unfocused 800 nm fs laser. The system proposed may be used for plasmonic dialysis of viruses *ex-vivo* in the blood flow of patients suffering from sepsis and/or an infectious disease, e.g. of the kidney. Further improvements of the method are the subject of a forthcoming work.

6. Conclusions

Results on formation and characterization of noble metal nanostructures created by pulsed laser ablation in vacuum are presented. Fs and ns laser systems are used in the experiments. Several methods for nanostructuring are employed and presented. Tuning of the composition and optical properties of the structures is achieved. The characterization includes several experimental techniques, while the theoretical study includes advanced simulation methods, as MD, FDTD and the GMM theory. Applications of the noble nanostructures obtained are described to SERS and biophotonics, namely, photo-thermal therapy of HeLa cancer and plasmonic optical tweezers.

References

[1] Glover T E, Ackerman G D, Lee R W and Young D A 2004 *Appl. Phys.* B **78/**7-8 995
[2] Glover T E 2003 *J. Opt. Soc. Am*. B **20/**10 125
[3] Amoruso S, Bruzzese R, Vitiello M, Nedialkov N N and Atanasov P A 2005 *J. Appl. Phys.* **98** 044907
[4] Lorazo P, Lewis L J and Meunier M 2006 *Phys. Rev.* B **73/**13 134108
[5] Nedialkov N N, Atanasov P A, Amoruso S, Bruzzese R and Wang X 2007 *Appl. Surf. Sci.* **253** 7761
[6] Amoruso S, Bruzzese R, Wang X, Nedialkov N N and Atanasov P A 2007 *J. Phys.* D*: Appl. Phys.* **40** 331
[7] Amoruso S, Bruzzese R, Wang X, Nedialkov N N and Atanasov P A 2007 *Nanotechnology* **18** 145612
[8] Allen M P and Tildesley D J 1987 *Computer Simulation of Liquids* (Clarendon Oxford)
[9] Girifalco L A and Weizer V G 1959 *Phys. Rev*. **114/**3 687
[10] Zhigilei L V and Garrison B J 1999 *Appl. Phys. Lett*. **74/**9 1341
[11] Taflove A 2005 *Computational Electromagnetics: The Finite-Difference Time-Domain Method*. (Boston, Artech House)
[12] Sullivan D M 2000 *Electromagnetic Simulation Using The FDTD Method* (New York, IEEE Press Series)
[13] Liu Z, Wei Q and Zhang X 2005 *Nano Letters* **5** 957
[14] Amoruso S, Nedyalkov N N, Wang X, Ausanio G, Bruzzese R and Atanasov P A 2011 *J. Appl. Phys.* **110** 124303
[15] Imamova S, Nedyalkov N, Dikovska A, Atanasov P, Sawczak M, Jendrzejewski R, Sliwinski G and Obara M 2010 *Appl. Surf. Sci.* **257** 1075
[16] Dikovska A Og, Nedyalkov N N and Atanasov P A 2011 *Materials Sci. Engin.* B **176** 1548
[17] Nedyalkov N N, Nikov Ru, Dikovska A Og, Atanasov P A, Obara G and Obara M 2012 *Appl. Surf. Sci*. **258** 9162
[18] Nikov Ru, Nedyalkov N, Atanasov P A, Terakawa M, Shimizu H and Obara M 2013 *Appl. Surf. Sci.* **264** 779
[19] Sakano T, Tanaka Y, Nishimura R, Nedyalkov N N, Atanasov P A, Saiki T and Obara M 2008 *J. Phys.* D*: Appl. Phys*. **41** 235304
[20] Nedyalkov N N, Imamova S E, Atanasov P A, Toshkova R A, Gardeva E G, Yossifova L S and Alexandrov M T 2010 *Comptes rendue de l'Acad. Bulg. des Sci*. **63/**5 767
[21] Hirano K, Shimizu H, Enami T, Terakawa M, Obara M, Nedyalkov N N and Atanasov P A 2013 *J. of Nanotech. in Diagnosis and Treatment* **1** 2